

# Predictions for multi-particle final states with SHERPA

T. GLEISBERG, S. HÖCHE, F. KRAUSS, A. SCHÄLICKE, S. SCHUMANN\*),  
G. SOFF, J. WINTER

*Institut für theoretische Physik, TU Dresden, D-01062 Dresden, Germany*  
*E-mail: steffen@theory.phy.tu-dresden.de*

Received 10 September 2004

In this contribution the new event generation framework **SHERPA** will be presented, which aims at a full simulation of events at current and future high-energy experiments. Some first results related to the production of weak vector bosons in association with jets at the Tevatron and the LHC will be discussed.

*PACS:* 13.85.-t, 13.85.Qk, 13.87.-a

*Key words:* Standard Model, Tevatron and LHC Physics, QCD

## 1 Introduction

Multi-particle and multi-jet final states will be of enormous importance at the LHC. They serve both as signals for interesting physics and as important backgrounds to many new physics channels. As an example for the first case, the production and decay of top quarks or SUSY particles can be mentioned. A typical background is the production of weak vector bosons in association with jets. The simulation of such processes is a great challenge that requires the development of new appropriate tools, for a recent review of these developments see [1]. The multi-purpose event generator **SHERPA** [2] is one of these new tools. As the re-writes of the well-established tools Pythia [3] and Herwig [4], namely Pythia7 [5] and Herwig++ [6], it is entirely written in the object-oriented programming language C++. One of the striking features of **SHERPA** is the inclusion of the CKKW prescription to combine tree-level multi-jet matrix elements with parton showers [7]. This method allows for a consistent description of multi-jet final states and a combination of such higher order calculations with the non-perturbative regime of hadron production in an universal manner. In Sec. 2 the generator **SHERPA** will be briefly reviewed. In Sec. 3 results obtained for the production of weak gauge bosons in association with jets at the Tevatron and the LHC will be presented.

## 2 The SHERPA generator

In its current version **SHERPA** is able to simulate electron–positron annihilations, unresolved interactions of photons with photons or leptons, and fully hadronic, i.e. proton–antiproton and proton–proton, collisions. Within **SHERPA** the different phases of the event simulation are hosted by physics-oriented modules. In its current version, **SHERPA-1.0.4** [8], the following physics modules are implemented:

---

\*) Talk given by S. Schumann at Physics at LHC, 13–17 July, 2004, Vienna, Austria.

X-sects (pb) $e^- \bar{\nu}_e + n$ QCD jets	Number of jets					
	0	1	2	3	4	5
AlpGen[18]	3904(6)	1013(2)	364(2)	136(1)	53.6(6)	21.6(2)
CompHEP[19]	3947.4(3)	1022.4(5)	364.4(4)			
GR@PPA[20]	3905(5)	1013(1)	361.0(7)	133.8(3)	53.8(1)	
MadEvent[21]	3902(5)	1012(2)	361(1)	135.5(3)	53.6(2)	
Sherpa	3908(3)	1011(2)	362(1)	137.5(5)	54(1)	

X-sects (pb) $e^- \bar{\nu}_e + b\bar{b}$	Number of jets				
	0	1	2	3	4
AlpGen	9.34(4)	9.85(6)	6.82(6)	4.18(7)	2.39(5)
CompHEP	9.415(5)	9.91(2)			
MadEvent	9.32(3)	9.74(1)	6.80(2)		
Sherpa	9.37(1)	9.86(2)	6.87(5)		

Table 1. Compilation of results for cross sections of some selected processes at the LHC. For details of the calculational setup and more results, cf. the MC4LHC homepage [17].

- Interface to various PDFs: CTEQ [9] and MRST [10] in their original form as well as many other PDFs through LHAPDF in its version 1 [11].
- AMEGIC++ [12] as generator for the matrix elements for hard scattering processes and decays as well as an internal library of analytical expressions for some very constrained set of  $2 \rightarrow 2$  processes. Besides the full SM, AMEGIC++ contains the full MSSM and an ADD model of large extra dimensions [13]. The SUSY particle spectra are provided by an interface to Isajet [14]. The next SHERPA release will in addition support the SUSY Les Houches accord interface [15]. AMEGIC++ has exhaustively been tested for a large number of production cross sections for six-body final states at an  $e^+e^-$  collider [16] and for various processes at the LHC, see Tab. 1 and [17].
- For multiple QCD bremsstrahlung, i.e. the emission of secondary partons, SHERPA’s own parton shower module APACIC++ [22] is invoked<sup>1</sup>). The merging of the hard matrix elements for multi-jet production and the subsequent parton showers is achieved according to the merging procedure proposed in [7], heavy quarks are treated with appropriate Sudakov form factors [24].
- Multiple parton interactions, giving rise to the “hard” underlying event, are currently being implemented. The corresponding module will be part of the next release of SHERPA.
- Hadronisation of the resulting partons and subsequent hadron decays so far are realized by an interface to the corresponding Pythia routines. However, a

<sup>1</sup>) In addition to the published version, it has been supplemented by parton showers in the initial state, enabling SHERPA to also simulate events with hadronic initial states [23].

new version of cluster fragmentation [25] is ready to be fully implemented in the near future.

### 3 Results for $W/Z$ +jets production

The production of electroweak gauge bosons, e.g.  $W^\pm$  and  $Z$  bosons, is one of the most prominent processes at hadron colliders. Through their leptonic decays, they leave a clean signature, namely either one charged lepton accompanied by missing energy for  $W$  bosons or two oppositely charged leptons for the  $Z$  bosons. The large statistics of these processes at the LHC will even allow the use of these channels as luminosity monitors. In addition these channels occur as important backgrounds to many signal processes. Due to the importance of these channels they were used to validate the merging procedure implemented in SHERPA and to compare the results with those of other approaches [26].

When merging matrix elements and parton showers according to the CKKW prescription the phase space for parton emission is divided into the hard region of jet production accounted for by suitable tree-level matrix elements and the softer region of jet evolution covered by the parton showers. Then, extra weights are applied on the former and vetoes on the latter, such that the overall dependence on the separation cut is minimal. The weight attached to the matrix elements takes into account the terms that would appear in a corresponding parton shower evolution. Therefore, a “shower history” is reconstructed by clustering the initial and final state particles stemming from the tree-level matrix element according to a  $k_\perp$ -formalism [27]. This procedure yields nodal values, namely the different  $k_\perp$ -measures  $Q^2$  where two jets have been merged into one. These nodal values can be interpreted as the relative transverse momentum describing the jet production or the parton splitting. The first ingredients of the ME weight are the strong coupling constants evaluated at the respective nodal values of the various parton splittings, divided by the value of the strong coupling constants as used in the evaluation of the matrix element. The other part of the correction weight is provided by suitable Sudakov form factors.

The first concern that has to be proven is that the dependence of the predictions on the merging scale  $Q_{\text{cut}}$  is small. Fig. 1 shows the transverse momentum distribution of the  $W^-$  boson and the corresponding electron in inclusive production at Tevatron Run II. The black solid line represents the total inclusive result as obtained with SHERPA. A vertical dashed line indicates the respective separation cut  $Q_{\text{cut}}$ , which has been varied between 10 GeV and 50 GeV. To guide the eye, all plots also show the same observable as obtained with a separation cut  $Q_{\text{cut}} = 20$  GeV, which is shown as a dashed black curve. The coloured lines give the contributions of different multiplicity processes. For the transverse momentum of the  $W$  below the cut, the distribution is dominated by the LO matrix element with no extra jet, i.e. the transverse momentum is generated by the initial state parton shower only. Around the cut, a small dip is visible. The  $p_\perp$  distribution of the electron, in contrast, is hardly altered. When looking on the rapidity distribution of the  $W$

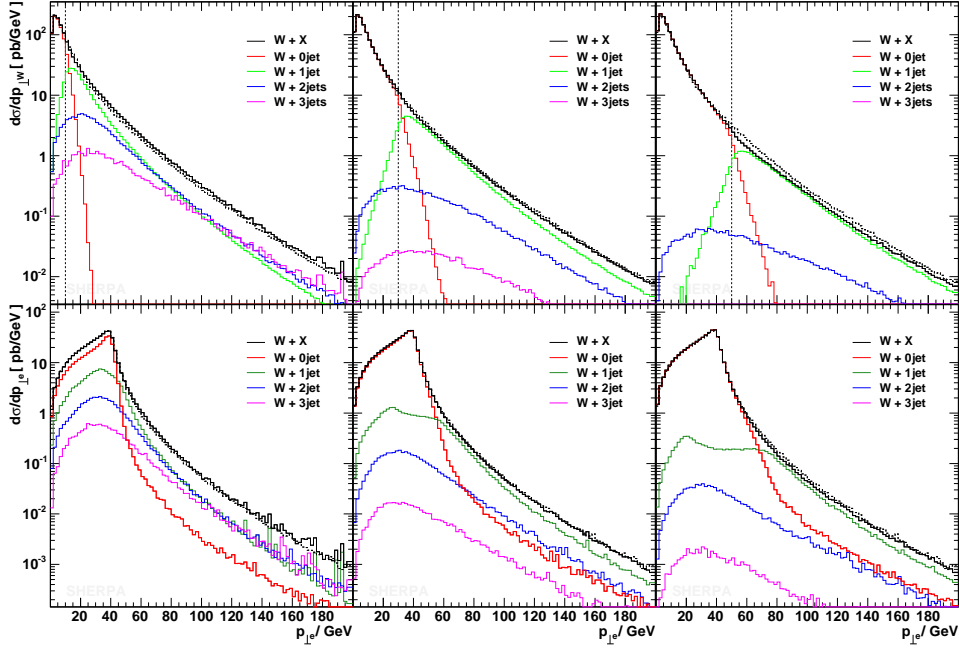


Fig. 1.  $p_{\perp}(W^{-})$  and  $p_{\perp}(e^{-})$  for  $Q_{\text{cut}} = 10$  GeV, 30 GeV and 50 GeV (black solid line) in comparison with  $Q_{\text{cut}} = 20$  GeV (black dashed line). The colored lines indicate the contributions of the different multiplicity processes.

boson and the electron, again to a very good approximation an independence on the merging scale has been observed.

In order to study the impact of the merging prescription, the predictions obtained with SHERPA have to be compared with other approaches. For  $W$  and  $Z$  plus jet production the results can be confronted with NLO QCD calculations delivered by the parton level generator MCFM [28]. In order to compare both approaches, a two-step procedure is chosen. In a first step the Sudakov and  $\alpha_s$  reweighted matrix elements are compared with exclusive NLO results obtained with MCFM. In the case of the next-to-leading order calculation, the exclusiveness of the final states boils down to a constraint on the phase space for the real parton emission. The exclusive SHERPA results consist of appropriate leading order matrix elements with scales set according to the  $k_{\perp}$ -clustering algorithm. The exclusiveness is achieved by suitable Sudakov form factors. In a second step, the jet spectra for inclusive production processes are compared. For the next-to-leading order calculation, this time the phase space for real parton emission is not restricted and the SHERPA predictions are obtained from a fully inclusive sample, using matrix elements with up to two extra jets and the parton showers attached. For the jet definition the Run II

$k_{\perp}$ -clustering algorithm defined in [29] is used.

In Fig. 2 the jet  $p_{\perp}$  distribution for the exclusive production of  $W+1$ jet and  $Z+2$ jets at Tevatron Run II are shown. In both figures, the SHERPA prediction is compared with the exclusive NLO result obtained with MCFM and with the naive LO prediction. For the fixed-order NLO and LO result, the renormalisation and factorisation scales have been set to  $\mu_R = \mu_F = M_W$ . All distributions have been normalised to the corresponding total cross section. This allows for a direct comparison of the distribution's shape. The change between the naive leading order and the next-to-leading order distribution is significant. At next-to-leading order the distributions become much softer. For a high- $p_{\perp}$  jet it is much more likely to emit a parton that fulfils the jet criteria and, therefore, the event is removed from the exclusive sample. The SHERPA predictions show the same feature. The inclusion of Sudakov form factors and the scale setting according to the merging prescription improves the LO prediction, leading to a rather good agreement with the next-to-leading order result.

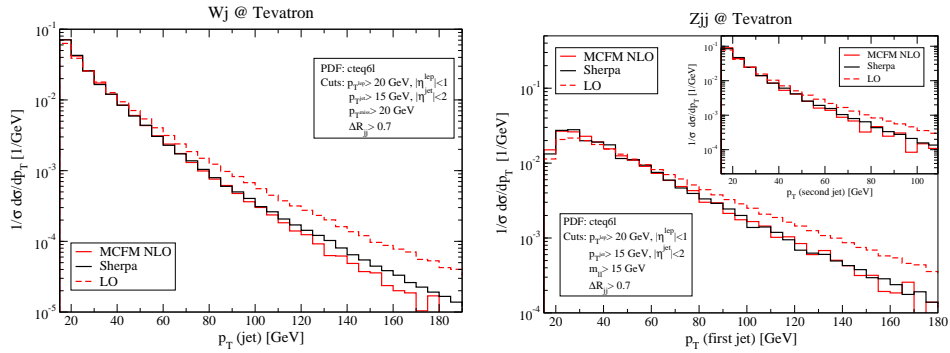


Fig. 2. The  $p_T$  distribution of the jet in exclusive  $W+1$ jet events (left) and the first and second jet in  $Z+2$ jet events (right) at Tevatron Run II. The SHERPA predictions are compared to the naive LO results and the corresponding NLO QCD predictions obtained with MCFM [28].

In Fig. 3 inclusive NLO results obtained with MCFM for the  $p_{\perp}$  of the hardest jet in  $W^++1$ jet and the hardest and second hardest jet in  $W^++2$ jets events at the LHC are compared to fully inclusive samples generated with SHERPA. There, the matrix elements for  $W/Z+0,1,2$ jet production have been used. The Sudakov and  $\alpha_s$  reweighted matrix elements have now been combined with the initial and final state parton showers. For both cases the SHERPA result and the NLO calculation are in good agreement.

Although it should be stressed that the rate predicted by SHERPA is still a leading order value only, a constant  $K$ -factor is sufficient to recover excellent agreement with a full next-to-leading order calculation for the distributions considered. Furthermore, by looking at the inclusive spectra it is obvious that this statement still

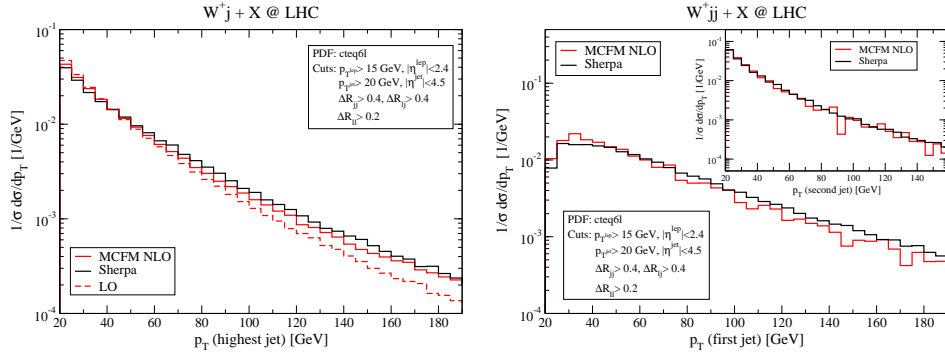


Fig. 3. The  $p_T$  distribution of the first jet in inclusive  $W^+ + 1\text{jet}$  (left panel) and the first and second jet in inclusive  $W + 2\text{jet}$  (right panel) production at the LHC. The SHERPA predictions are compared to the corresponding NLO QCD prediction obtained with MCFM [28]. For the naive LO and the NLO calculation the renormalisation and factorisation scale has been set to  $\mu_R = \mu_F = M_W$ .

holds true after the inclusion of parton showers and the merging of exclusive matrix elements of different jet multiplicities.

Finally, a comparison of the SHERPA predictions with experimental data provides an ultimate test of SHERPA's ability to describe  $W$  and  $Z$  production at hadron colliders. In Fig. 4, the (inclusive)  $p_\perp$  distribution of the  $W$  and  $Z$  boson is compared with data from D0 [30] and CDF [31], respectively, taken at Run I of the Tevatron. After a rescaling of the SHERPA predictions by constant  $K$ -factors the agreement with data for both distributions is excellent.

#### 4 Conclusions

The results presented for the production of  $W$  and  $Z$  bosons at hadron colliders prove that the merging of tree-level matrix elements and parton showers as implemented in SHERPA is working in a systematically correct manner; further tests will include, e.g., the sensitivity of results to the choice of scale, the quality in describing more complicated correlations, for instance of different jets and the simulation of more processes. This agenda currently is being worked on, the first results being very encouraging. This indicates that SHERPA is perfectly suitable to meet the enhanced demands of the community to reliably simulate physics processes at the next generation of collider experiments.

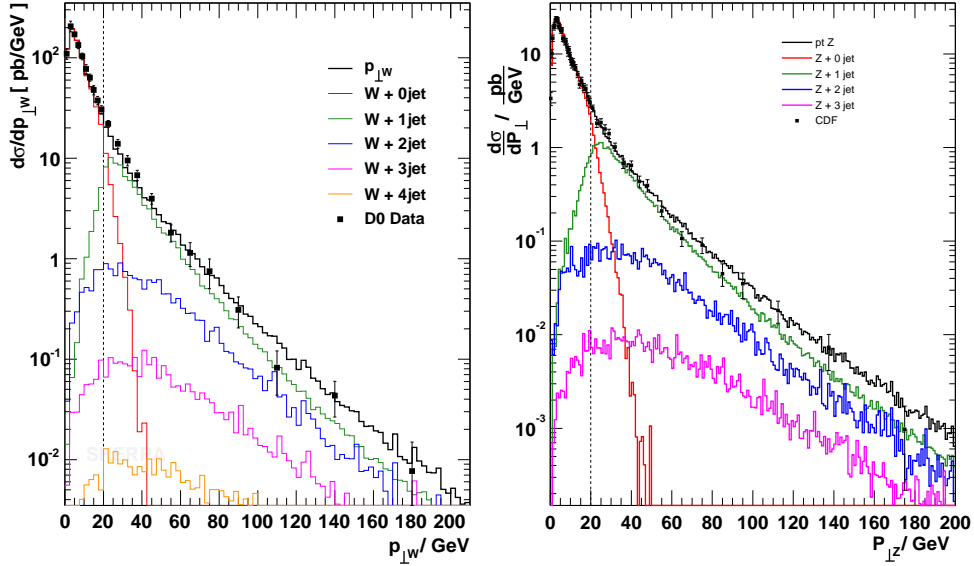


Fig. 4. The  $p_{\perp}$  distributions of the  $W$  (left panel) and  $Z$  boson (right panel) in comparison with Tevatron Run I D0 data [30] and CDF data [31], respectively. The total results are indicated by the black lines. The colored lines show the contributions of the different multiplicity processes. The applied separation cut for both samples is  $Q_{\text{cut}} = 20$  GeV.

### Acknowledgments

The authors gratefully acknowledge financial support by BMBF, DFG, and GSI. S.S. wishes to thank the organisers of “Physics at LHC” for the extremely pleasant atmosphere and fruitful discussions during the conference and the financial support provided.

### References

- [1] M. L. Mangano, eConf **C030614** (2003) 015 [arXiv:hep-ph/0312117].
- [2] T. Gleisberg, S. Höche, F. Krauss, A. Schälicke, S. Schumann and J. C. Winter, JHEP **0402** (2004) 056.
- [3] T. Sjöstrand, P. Eden, C. Friberg, L. Lönnblad, G. Miu, S. Mrenna and E. Norrbin, Comput. Phys. Commun. **135** (2001) 238;  
T. Sjöstrand, L. Lönnblad, S. Mrenna, P. Skands, arXiv:hep-ph/0308153.
- [4] G. Corcella *et al.*, JHEP **0101** (2001) 010; G. Corcella *et al.*, arXiv:hep-ph/0210213.

- [5] M. Bertini, L. Lönnblad and T. Sjöstrand, *Comput. Phys. Commun.* **134** (2001) 365.
- [6] S. Gieseke, A. Ribon, M. H. Seymour, P. Stephens and B. Webber, *JHEP* **0402**, 005 (2004).
- [7] S. Catani, F. Krauss, R. Kuhn and B. R. Webber, *JHEP* **0111** (2001) 063; F. Krauss, *JHEP* **0208** (2002) 015.
- [8] To download the program see: <http://www.physik.tu-dresden.de/~krauss/hep>.
- [9] J. Pumplin, D. R. Stump, J. Huston, H. L. Lai, P. Nadolsky and W. K. Tung, *JHEP* **0207** (2002) 012.
- [10] A. D. Martin, R. G. Roberts, W. J. Stirling and R. S. Thorne, *Eur. Phys. J. C* **14** (2000) 133.
- [11] See the homepage: <http://vircol.fnal.gov/>.
- [12] F. Krauss, R. Kuhn and G. Soff, *JHEP* **0202** (2002) 044.
- [13] T. Gleisberg, F. Krauss, K. T. Matchev, A. Schälicke, S. Schumann and G. Soff, *JHEP* **0309** (2003) 001.
- [14] H. Baer, F. E. Paige and S. D. Protopopescu, and X. Tata, arXiv:hep-ph/0001086.
- [15] P. Skands *et al.*, *JHEP* **0407** (2004) 036.
- [16] T. Gleisberg, F. Krauss, C. G. Papadopoulos, A. Schälicke and S. Schumann, *Eur. Phys. J. C* **34** (2004) 173.
- [17] <http://mlm.home.cern.ch/mlm/mcwshop03/mcwshop.html>
- [18] M. L. Mangano, M. Moretti, F. Piccinini, R. Pittau and A. D. Polosa, *JHEP* **0307** (2003) 001.
- [19] A. Pukhov *et al.*, arXiv:hep-ph/9908288.
- [20] K. Sato *et al.*, Proc. VII International Workshop on Advanced Computing and Analysis Techniques in Physics Research (ACAT 2000), P. C. Bhat and M. Kasemann, AIP Conference Proceedings **583** (2001) 214.
- [21] T. Stelzer and W. F. Long, *Comput. Phys. Commun.* **81** (1994) 357; F. Maltoni and T. Stelzer, *JHEP* **0302** (2003) 027.
- [22] R. Kuhn, F. Krauss, B. Ivanyi and G. Soff, *Comput. Phys. Commun.* **134** (2001) 223.
- [23] F. Krauss, A. Schälicke and G. Soff, in preparation.
- [24] F. Krauss and G. Rodrigo, *Phys. Lett. B* **576** (2003) 135.
- [25] J. C. Winter, F. Krauss and G. Soff, *Eur. Phys. J. C* **36** (2004) 381.
- [26] F. Krauss, A. Schälicke, S. Schumann and S. Soff, arXiv:hep-ph/0409106.
- [27] S. Catani, Y. L. Dokshitzer and B. R. Webber, *Phys. Lett. B* **285** (1992) 291; S. Catani, Y. L. Dokshitzer, M. H. Seymour and B. R. Webber, *Nucl. Phys. B* **406** (1993) 187.
- [28] J. Campbell and R. K. Ellis, *Phys. Rev. D* **65** (2002) 113007; J. Campbell, R. K. Ellis and D. L. Rainwater, *Phys. Rev. D* **68** (2003) 094021.
- [29] G. C. Blazey *et al.*, arXiv:hep-ex/0005012.
- [30] B. Abbott *et al.* [D0 Collaboration], *Phys. Lett. B* **513** (2001) 292.
- [31] T. Affolder *et al.* [CDF Collaboration], *Phys. Rev. Lett.* **84** (2000) 845.